Efficacy, safety and novel targets in cardiovascular disease : advanced applications in APOE*3-Leiden.CETP mice

Pouwer, M.G.


4

The BCR-ABL1 inhibitors imatinib and ponatinib decrease plasma cholesterol and atherosclerosis, and nilotinib and ponatinib activate coagulation in a translational mouse model

Marianne G. Pouwer, Elsbet J. Pieterman, Lars Verschuren,
Martien P. M. Caspers, Cornelis Kluft, Ricardo A. Garcia, Jurjan Aman,
J. Wouter Jukema, Hans M. G. Princen

Front Cardiovasc Med. 2018 Jun 12;5:55

Abstract

Objectives: Treatment with the second and third generation BCR-ABL1 tyrosine kinase inhibitors (TKIs) increases cardiovascular risk in chronic myeloid leukemia (CML) patients.
Methods and results: We investigated the vascular adverse effects of three generations of TKIs in a translational model for atherosclerosis, the APOE*3-Leiden.CETP mouse. Mice were treated for sixteen weeks with imatinib (150 mg/kg BID), nilotinib (10 and 30 mg/kg QD) or ponatinib (3 and 10 mg/kg QD), giving similar drug exposures as in CML-patients. Cardiovascular risk factors were analyzed longitudinally, and histopathological analysis of atherosclerosis and transcriptome analysis of the liver was performed. Imatinib and ponatinib decreased plasma cholesterol (imatinib, −69%, $p<0.001$; ponatinib 3 mg/kg, −37%, $p<0.001$; ponatinib 10 mg/kg, −44%, $p<0.001$) and atherosclerotic lesion area (imatinib, −78%, $p<0.001$; ponatinib 3 mg/kg, −52%, $p=0.002$; ponatinib 10 mg/kg, −48%, $p=0.006$), which were not affected by nilotinib. In addition, imatinib increased plaque stability. Gene expression and pathway analysis demonstrated that ponatinib enhanced the mRNA expression of coagulation factors of both the contact activation (intrinsic) and tissue factor (extrinsic) pathways. In line with this, ponatinib enhanced plasma levels of FVII, whereas nilotinib increased plasma FVIIa activity.
Conclusions: While imatinib showed a beneficial cardiovascular risk profile, nilotinib and ponatinib increased the cardiovascular risk through induction of a pro-thrombotic state.

Introduction

Chronic myeloid leukemia (CML) is a myeloproliferative neoplasm caused by a translocation of the chromosomes 9 and 22 that results in formation of the Bcr-Abl1 oncogene (1) and a constitutively active c-Abl kinase domain, which drives uncontrolled cell growth and tumorigenesis.

Patients with CML are treated with specific tyrosine kinase inhibitors (TKIs). The first-line TKI imatinib is widely used and has proven to be successful in the treatment of CML. However, relapses are seen in up to 17% of patients treated with imatinib (2) due to amplification and mutations in the Bcr-Abl1 gene (3) that lead to imatinib resistance. The second and third generation TKIs, nilotinib and ponatinib among others, are effective against these mutations (3), and promising results have been found in relapsed patients (4). Unfortunately, side effects have been reported in patients receiving these TKIs including myocardial infarction and progressive arterial occlusive disease (PAOD) (5–7). As a result, ponatinib was temporarily removed from the US market, and was later reintroduced for the treatment of patients with T315I-positive CML or those in whom no other TKI was indicated.

Since the first reports of vascular adverse effects (VAEs), many authors related the adverse effects of TKI treatment to atherosclerosis and abnormal platelet function (4,7–9). However, it is still unclear whether the side effects are caused by enhanced vascular inflammation and endothelial dysfunction, atherosclerosis development, increased thrombotic activity per se, or a combination of these processes. Furthermore, the underlying disease has been reported to affect metabolic parameters (10) and coagulation (11), which may interfere with the onset of the side-effects upon treatment. Therefore, to elucidate the role of TKI treatment on VAE's independently of a background of leukemia, we performed a detailed experimental study in healthy pro-atherogenic mice. The aim of this study was to assess the (cardio)vascular side effects of the second and third generation of TKIs, nilotinib and ponatinib, and to compare their effects to the first generation TKI imatinib.

In this study, we used the APOE*3-Leiden.CETP mouse as a well-established model for dyslipidemia and atherosclerosis, with a human-like lipoprotein metabolism and atherosclerosis development. These mice show a human-like response to all lipid-modulating interventions that are being used in the clinic (12–18) and have been used previously to investigate the underlying mechanism of cardiovascular safety issues (19).

We found that imatinib and ponatinib decreased plasma cholesterol, which was associated with decreased atherosclerosis development. Gene expression and pathway analysis demonstrated adverse alterations in genes involved in coagulation which were in line with increased plasma levels of FVII and FVIIa by ponatinib and nilotinib respectively, pointing towards thrombosis instead of atherosclerosis as inducer of the VAEs.

Materials and methods

Animals

Female APOE*3-Leiden.CETP transgenic mice (9 to 14 weeks of age) from the SPF breeding stock at TNO-Metabolic Health Research (TNO-Leiden) were used in this study. Females were used because they are more responsive to dietary cholesterol and fat than males. APOE*3-Leiden females have a higher VLDL production (20) than males resulting in higher plasma total cholesterol (TC) and triglyceride (TG) levels and more pronounced development of atherosclerosis (21,22). During the study, mice were housed under standard conditions with a 12 h light-dark cycle and had free access to food and water. Body weight, food intake and clinical signs of behavior were monitored regularly during the study. Animal experiments were approved by the Institutional Animal Care and Use Committee of The Netherlands Organization for Applied Research under registration number 3557.

Experimental design and analyses

Mice were fed a semi-synthetic diet, containing saturated fat from 15% (w/w) cacao butter and 0.15% cholesterol (Western-type diet [WTD]; Hope Farms, Woerden, The Netherlands). All studies started after a run-in period of 3 weeks on WTD, which is designated as t=0 weeks/baseline, after which mice were matched into groups based on body weight, total cholesterol (TC), plasma triglycerides (TG) and age. For the pharmacokinetic (PK) study, mice were randomized in 3 groups (n=9 per group) and received a single oral gavage with imatinib (100 mg/kg), nilotinib (50 mg/kg) or ponatinib (5 mg/kg). At 0.5, 1 and 2 h after oral gavage, blood was sampled from 3 mice per group per time point, and at 4, 7 and 24 h blood was collected by heart puncture after sacrifice. For the (cardio)vascular risk factor and atherosclerosis study, mice were randomized in 6 groups (n=15 per group, n=20 in control group) and received, based on the results of the PK study, a once-daily oral gavage with nilotinib (10 or 30 mg/kg), ponatinib (3 or 10 mg/kg), or a twice-daily gavage with imatinib (150 mg/kg). The TKIs were suspended in 5% carboxymethyl cellulose and all mice except the imatinib group received a second oral gavage with the vehicle alone (5% carboxymethyl cellulose). The TKIs were purchased at LC laboratories, Woburn (MA), USA. After 12 weeks 5 mice of the control group were sacrificed to asses atherosclerosis development and to determine the end-point of the study. After sixteen weeks of treatment all animals were sacrificed by CO_2 inhalation. Plasma cholesterol, TG, high-density lipoprotein cholesterol (HDL-C), lipoprotein profiles, serum amyloid A (SAA), E-selectin and monocyte chemoattractant protein 1 (MCP-1), aspartate transaminase (AST) and alanine transaminase (ALT) were measured throughout the study. Blood pressure was measured at 2 and 15 weeks of treatment. Measurement of hepatic lipid and protein content; protein and albumin content in broncho-alveolar lavage (BAL) fluid; urinary albumin/creatinine levels; and histology of lung and hearts was performed at 16 weeks. Total FVII coagulant

activity was measured at 4 and 12 weeks and FVIIa activity at 4 weeks. Gene expression analysis using Next Generation Sequencing with the Illumina Nextseq 500 and subsequent pathway analysis of liver of 8 mice per group was performed following established protocols (23,24).

PK analysis and plasma drug concentrations

EDTA plasma samples collected during the 24-hour PK study and at week 16 of the (cardio) vascular risk factor-atherosclerosis study were subsequently stored at -80°C until analysis. Thawed plasma samples (50 µL) were de-proteinized with two volumes of acetonitrile containing an appropriate src-inhibitor chemotype as internal standard for each analyte. Following deproteinization, a 5 µL portion of clear supernatant was then subjected to solvent gradient separation in an Agilent 1100 series HPLC system interfaced to a Micromass triple-quadrupole mass spectrometer, which was operated in the positive ion electrospray MRM mode to obtain daughter ions for quantitation: Ion transitions used for quantitation were as follows: imatinib [494.3 -> 394.2], nilotinib [530.2 -> 289.2], ponatinib [533.3 -> 260.3]. Standard curves ranging from 1 nM to 6 µM were fitted with a quadratic regression weighted by reciprocal concentration (1/x). LLOQ for the purposes of this assay was between 1 and 2 nM for all compounds analyzed. QC samples at three levels in the range of the standard curve were used to accept individual analytical sets, and all results were calculated as the mean of triplicate determinations ± standard error. T_{max}, C_{max} and AUCs were calculated using the software Berkeley Madonna (version 8.3.18).

Biochemical analyses and blood pressure

EDTA plasma samples were collected throughout the study. Plasma cholesterol and triglycerides were determined every 4 weeks using enzymatic kits (Roche/Hitachi) according to the manufacturer's protocols and average plasma levels over week 4 to 16 were calculated. HDL-C was measured after precipitation as described previously (17). The distribution of cholesterol over plasma lipoproteins was determined in group wise-pooled plasma by fast protein liquid chromatography (FPLC) (25). The inflammatory markers SAA, E-selectin and MCP-1 were measured using the ELISA kits from Tridelta (SAA) and R&D (MCP-1, E-selectin) according to the manufacturer's instruction. Plasma ALT and AST were determined using a spectrophotometric assay (Boehringer Reflotron system) in group wise-pooled samples. Systolic blood pressure (SBP), diastolic blood pressure (DBP) and heart rate were measured using the tail cuff method in 8 mice per group at 2 and 15 weeks (26).

Hepatic lipid analysis

Livers were isolated and partly homogenized (30 s at 5000 rpm) in saline (~10% wet wt/vol) using a mini-bead beater (Biospec Products, Inc., Bartlesville, OK). Lipids were extracted as described (27) previously and separated by high-performance thin-layer chromatography (HPTLC). Lipid spots were stained with color reagent (5 g $MnCl_{2\cdot4}H_2O$, 32 mL 95–97%

H_2SO_4 added to 960 mL of CH_3OH:H_2O 1:1 vol/vol) and quantified using TINA version 2.09 software (Raytest, Straubenhardt, Germany) (27).

BAL and urinary albumin/creatinine

The lungs were flushed two times with 750 µL PBS into the trachea using a BD 20G angio-catheter to collect broncho-alveolar lavage (BAL) fluid. Protein and albumin content in BAL fluid were determined in the supernatant using the protein determination kit from Pierce and the mouse albumin ELISA kit (ALPCO, Salem, USA). Urinary albumin and creatinine levels were determined using the mouse albumin ELISA kit (ALPCO, Salem, USA) and the creatinine kit (Exocell, Philadelphia, USA) according to manufacturer's instruction.

Flow cytometric analysis

White cell profiling was performed via fluorescence activated cell sorting (FACS) using the BD FACS Canto II apparatus (Becton Dickinson, Franklin Lakes, New Jersey, USA). After 12 weeks of treatment, peripheral blood mononuclear cells (PBMCs) were isolated from fresh blood samples of 8 mice per group, and were sorted into CD11b+/CD11c- (monocytes), and further divided into CD11b+/Ly6C^{Low} and CD11b+/Ly6C^{High} monocytes. The following conjugated monoclonal antibodies, all from eBiosciences, were used: CD11b-FITC, CD11c-PE/Cy7, Ly6C-APC.

Coagulation factor VII and VIIa

Total clotting FVII and FVIIa activity were measured on a STA compact apparatus (Diagnostica Stago Inc. Parsippany, NJ). For the determination of total clotting FVII a one stage Prothrombin assay with Dade Innovin PT reagent (Siemens) and Hemoclot FVII reagent (Hyphen Biomed) as deficient agent were used and calibration was performed with pooled normal mouse plasma. Staclot VIIa rTF (Diagnostica Stago Inc.) and Hemoclot FVII reagent (Hyphen Biomed) were used to determine FVIIa activity, calibrated with Novoseven® (Novonordisk).

Histological assessment of lung morphology and atherosclerosis

Tissues were isolated, fixed in formalin, and embedded in paraffin. The caudal lung was cross sectioned (3 µm thick) and stained with hematoxylin-eosin (HE), Sirius Red for collagen, and with isolectin B4 (1:50; Sigma-Aldrich, Missouri, USA) for endothelial cells. Hearts were sectioned perpendicular to the axis of the aorta, starting within the heart and working in the direction of the aortic arch. Once the aortic root was identified by the appearance of aortic valve leaflets and smooth muscle cells instead of collagen-rich tissue, serial cross sections (5 µm thick with intervals of 50 µm) were taken and mounted on AAS-coated slides. These sections were stained with hematoxylin-phloxine-saffron (HPS) for histological analysis. For each mouse, atherosclerosis was measured in 4 subsequent cross-sections. Each section consisted of 3 segments. The average total lesion area per

cross-section was then calculated (17,28). For determination of lesion severity the lesions were classified into five categories according to the American Heart Association classification (29): 0) no lesion I) early fatty streak, II) regular fatty streak, III) mild plaque, IV) moderate plaque, and V) severe plaque. The percentage of each lesion type was calculated, where type I-III lesions were classified as mild lesions and type IV-V lesions were classified as severe lesions (17,28). In the aortic root, lesion composition was determined for the severe lesions (type IV-V) as a percentage of lesion area after immunostaining with anti-human alpha-actin (1:400; PROGEN Biotechnik GmbH, Germany) for smooth muscle cells (SMC), and anti-mouse Mac-3 (1:50; BD Pharmingen, the Netherlands) for macrophages followed by Sirius Red staining. After Sirius Red staining for collagen, color intensity was determined in ImageJ and the used threshold was confirmed by evaluation of the sections under polarized light (30). Necrotic area and cholesterol clefts were measured after HPS staining (17,28,31). Lesion stability index was calculated as described previously (17,31). In each segment used for lesion quantification, the number of monocytes adhering to the endothelium were counted after immunostaining with AIA 31240 antibody (1:1000; Accurate Chemical and Scientific, New York, New York, USA) (16,17).

Gene expression analysis

Messenger RNA was isolated from liver of 8 mice per group, using the NEBNext Ultra RNA sample Prep Kit. After fragmentation of the mRNA, cDNA synthesis was performed. The quality and yield after sample preparation was measured with the Fragment Analyzer. Clustering and DNA sequencing was performed using the Illumina Nextseq 500. The genome reference and annotation file Mus_Musculus.GRCm38 was used for analysis in FastA and GTF format. The reads were aligned to the reference sequence using Tophat 2.0.14 combined with Bowtie 2.1.0, and based on the mapped read locations and the gene annotation HTSeq-count version 0.6.1p1 was used to count how often a read was mapped on the transcript region. Calculated p-values <0.01 were used as threshold for significance. Selected differentially expressed genes (DEGs) were used as an input for pathway analysis through Ingenuity Pathway Analysis (IPA) suite (www.ingenuity.com, accessed 2015). Gene set enrichment analysis was used to highlight the most important processes and pathways. Relevance of these pathways and processes is indicated as p-value and visualized in a graph by calculating the –log(p-value).

Statistical analysis

Significance of differences between the groups was calculated in SPSS 22.0 for Windows. Normally distributed data was tested parametrically using a one-way ANOVA for multiple comparisons with a Dunnett's post-hoc test. Non-parametric data were compared separately with a Mann-Whitney U test with adjusted rejection criteria using a Bonferroni-Holm correction. Correlations between lesion size (after square root transformation) and cholesterol exposure were calculated with a Pearson's correlation test. All groups

were compared with the control group. Values are presented as means ± SD and p-values <0.05 were considered statistically significant.

Results

PK analysis and plasma drug concentrations

Pharmacokinetic analysis was performed after a single dose of imatinib (100 mg/kg), nilotinib (50 mg/kg) or ponatinib (5 mg/kg) (**Table 1**) and based on these results the doses for the atherosclerosis study were adjusted to twice daily 150 mg/kg for imatinib, once daily 10 or 30 mg/kg for nilotinib and once daily 3 or 10 mg/kg for ponatinib. The relatively high dose of imatinib needed to achieve plasma concentrations comparable to those in CML-patients was due to the short half-life of the drug in mice and is in line with previous reports (32). Drug exposure after repeated dosing was measured in sacrifice plasma and calculated AUCs were similar to those in CML-patients for imatinib and the low doses of nilotinib and ponatinib (**Table 1**).

Safety aspects of treatments with TKIs

No clinical signs of deviant behavior and no effects on body weight and food intake were noted in any treatment group as compared with control. Plasma ALT and AST, measured at the start and after 16 weeks of treatment, showed no aberrant results (**Table 2**). The number of circulating peripheral blood mononuclear cells (PBMC's) in the blood as measured by FACS analysis at 12 weeks (**Table 2**) was reduced by imatinib (–42%, p=0.006) and by the high-dose ponatinib (–44%, p=0.003). In addition, imatinib and the high doses of nilotinib and ponatinib decreased pro-inflammatory $Ly6C^{High}$ monocytes, all consistent with the mode of action of TKIs. Two mice (ponatinib 3 mg/kg) died during blood pressure measurements at t=15 weeks, and one mouse (nilotinib 30 mg/kg) was excluded from atherosclerosis measurement due to deviating heart anatomy.

(Cardio) vascular risk factors

Imatinib and ponatinib reduce plasma cholesterol levels

As dyslipidemia is a major risk factor for cardiovascular disease, we measured plasma cholesterol and triglyceride levels throughout the study, and HDL-C at the end point. The WTD resulted in an average plasma cholesterol of 17.3 ± 3.5 mmol/L, TGs of 3.3 ± 1.0 mmol/L, and an HDL-C level of 1.4 ± 0.2 mmol/L in the control group. When compared to the control group, imatinib reduced average cholesterol and TG levels by 69% (p<0.001) and 36% (p=0.019), respectively. Ponatinib decreased cholesterol levels by 37% (3 mg/kg, p<0.001) and 44% (10 mg/kg, p<0.001), whereas nilotinib had no significant effect on plasma lipid levels (**Figure 1A–D**). At 16 weeks of treatment, HDL-C was decreased by ponatinib in both the low (–30%, p=0.003) and high (–25%, p=0.016) dose. The reduction

Table 1 Pharmacokinetics of imatinib, nilotinib and ponatinib in APOE*3-Leiden.CETP mice and CML-patients

TKI	APOE*3-Leiden.CETP mice					CML patients				
	Dose (mg/kg)		T_{max} (h)	C_{max} (µg/mL)	AUC_{0-24} (µg/mL*h)	Dose (mg/kg)		subject	AUC_{0-24} (µg/mL*h)	reference
Imatinib	Single	100	2.28	5.29	32.79	Day 1, BID	400	CML-patients	36.2 ± 7.4	(33)
	Repeated dose, BID	150	2.47	11.07	78.13	Steady state, BID	400	CML-patients	68.4 ± 29.8	(33)
Nilotinib	Single	50	3.26	10.97	117.49	Single, QD	400	Healthy subjects	14.7 ± 5.0	(34)
	Repeated dose, QD	10	3.17	2.30	24.60	Repeated dose, QD	400-1200	CML-patients	36.0 ± 11.8	(34)
	Repeated dose, QD	30	3.17	6.89	73.81					
Ponatnib	Single	5	8.00	0.19	3.24	Single, QD	60	CML-patients	0.7 ± 0.4	(35)
	Repeated dose, QD	3	6.72	0.14	2.43	Repeated dose, QD	15-60	CML-patients	1.3	(36)

T_{max}, C_{max} and AUC_{0-24} were calculated after a single dose or after 16 weeks of treatment (repeated dose) for imatinib, nilotinib and ponatinib and compared with plasma concentrations in CML patients. Data are presented as means (APOE*3-Leiden.CETP mice) and means ± SD (CML-patients), unless SD was not given in the reports. Abbreviations: AUC, area under the curve; BID, twice a day; CML, chronic myeloid leukemia; QD, once a day.

Table 2 Safety aspects of TKI treatment, the number of PBMCs and the fraction CD11b+Ly6C$^{High/Low}$ monocytes. Body weight, food intake (per cage) plasma ALT (pooled), and plasma AST (pooled) at baseline and after 16 weeks of treatment with imatinib (150 mg/kg, BID), nilotinib (10 and 30 mg/kg) or ponatinib (3 and 10 mg/kg). After 12 weeks, FACS analysis was performed.

	Dose	Body weight	Food intake	ALT	AST	Number of live/single PBMCs per mL blood	% of monocyte population	
	mg/kg	*gram*	*gram/mouse/day*	*U/L*	*U/L*	*(*10^6/mL)*	**CD11b+Ly6C^{High}**	**CD11b+Ly6C^{Low}**
Baseline	-	21.6 ± 1.7	3.0	57	163	-	-	-
Control	-	23.3 ± 2.4	2.5	54	224	6.8 ± 1.3	19.0 ± 4.4	71.7 ± 3.9
Imatinib	150	22.1 ± 0.8	2.6	31	147	3.9 ± 1.3**	11.0 ± 3.6**	69.1 ± 5.9
Nilotinib	10	22.5 ± 1.5	2.3	64	210	6.5 ± 2.4	27.5 ± 4.3	61.4 ± 4.8
	30	22.2 ± 1.3	2.4	81	221	6.4 ± 1.4	11.4 ± 3.8*	73.2 ± 4.9
Ponatinib	3	22.5 ± 2.3	2.4	44	196	7.1 ± 1.7	26.1 ± 2.9	58.4 ± 2.5
	10	22.3 ± 2.8	2.3	31	207	3.8 ± 0.8**	12.6 ± 3.1*	69.1 ± 6.4

Data are presented as means ± SD (n=13-15 per group; n=7-8 per group for FACS analysis) or as means (cage or group level) (n=2-4 mice per cage).
*p<0.05, **p<0.01 as compared to control. Abbreviations: ALT, Alanine transaminase; AST, aspartate transaminase; PBMCs, peripheral blood mononuclear cells.

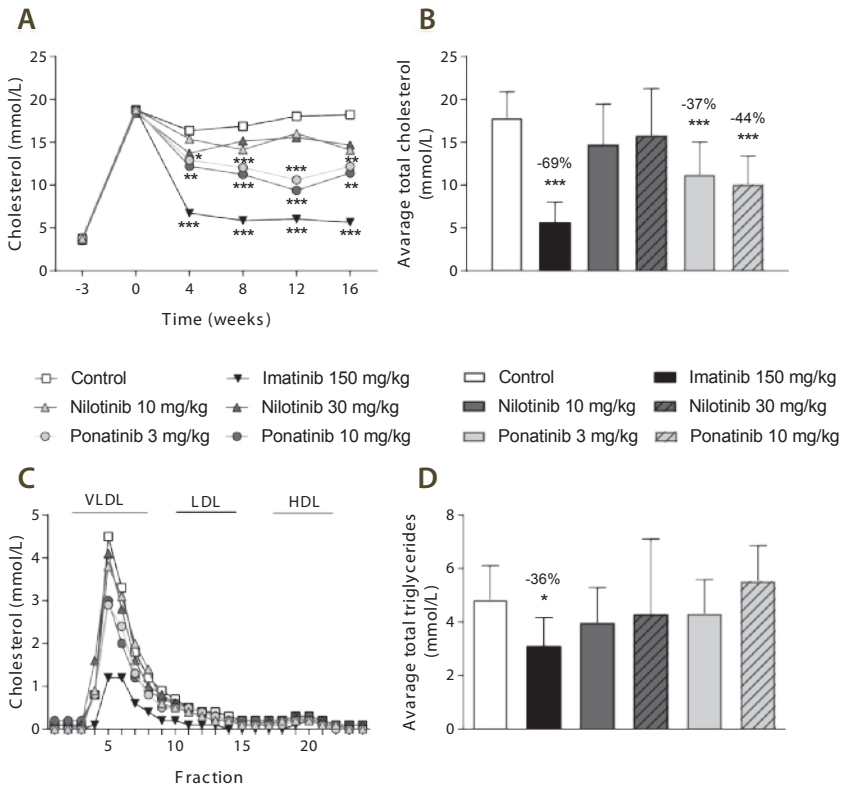

Figure 1 Imatinib and ponatinib reduce plasma cholesterol levels and imatinib decreases average TGs. Plasma cholesterol was measured throughout the 16 week study (A) and average plasma cholesterol (B) and TGs (D) were calculated. Lipoprotein profiles were assessed by FPLC lipoprotein separation after 16 weeks of treatment (C). Data are presented as means ± SD (n = 13–15 per group). *p < 0.05, **p < 0.01 ***p < 0.001. Abbreviations: FPLC, Fast protein liquid chromatography; VLDL, very-low-density-lipoprotein; LDL, low-densitylipoprotein; HDL, high-density-lipoprotein; TGs, triglycerides.

of plasma cholesterol by imatinib and ponatinib was mainly confined to VLDL-LDL (i.e., non-HDL) (**Figure 1C**). These findings show that imatinib decreases plasma cholesterol and TG levels in APOE*3-Leiden.CETP mice, which is consistent with the cholesterol-lowering effect observed in patients (37–40).

Ponatinib and imatinib decrease hepatic lipid content

Liver lipid storage may give insight into how lipid metabolism is affected by imatinib and ponatinib. Therefore, hepatic lipid content was measured by HPTLC. Free cholesterol

content was decreased by 10 mg/kg ponatinib (–21%, p=0.007) (**Figure 2A**), cholesterol ester content was decreased by imatinib (–30%, p=0.001) and by both the low (–49%, p<0.001) and high (–61%, p<0.001) dose of ponatinib (**Figure 2B**). TG content was decreased by the low (–32%, p=0.048) and high (–43%, p=0.005) dose of ponatinib (**Figure 2C**). These data point to a shortage of cholesterol in the liver and suggest that not cholesterol clearance, but VLDL production and/or intestinal absorption of cholesterol are affected by ponatinib and imatinib.

Blood pressure and vascular dysfunction

Increased blood pressure and endothelial activation may lead to vascular dysfunction and atherosclerosis. SBP, measured after 2 and 15 weeks of treatment, was 91 ± 7 and 86 ± 5 mmHg, respectively, in the control group, and heart rate was 726 ± 46 and 716 ± 29 beats per minute. SBP and heart rate were not affected by imatinib, nilotinib or ponatinib treatment. As markers of vascular integrity and leakage or edema formation, we evaluated lung histology, determined the wet/dry weight ratio of the lungs and measured the amount of protein in the BAL fluid. None of the anti-CML drugs showed significant effects on histology and wet/dry weight ratio (data not shown), and ponatinib decreased the amount of protein in BAL fluid by 51% (3 mg/kg, p=0.029) and by 47% (10 mg/kg, p=0.041) (**Table 3**). In contrast, ponatinib increased the urinary albumin/creatinine ratio (approximately 13-fold, N.S.), mainly due to 3 mice with very high levels of urinary albumin (**Table 3**). These data indicate that the anti-CML drugs did not cause damage to the microvasculature in the lungs but that ponatinib may lead to microvascular dysfunction in the kidney.

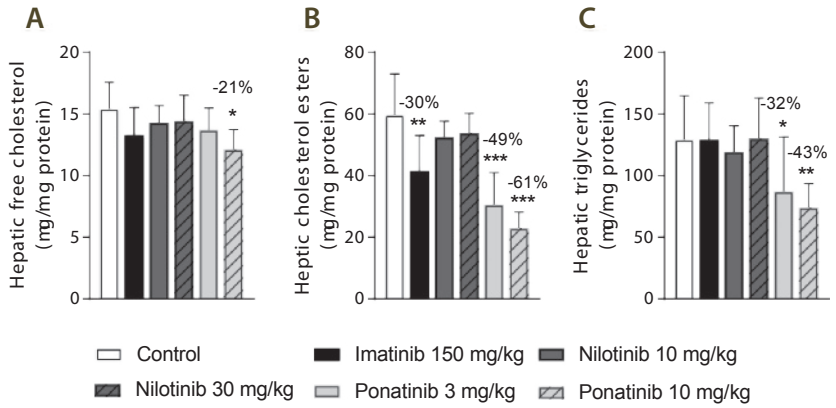

Figure 2 Imatinib and ponatinib decrease hepatic lipid content. Hepatic free cholesterol (A), cholesterol ester (B) and triglyceride (C) content were measured by HPTLC after 16 weeks of treatment. Data are presented as means ± SD (n=8 per group).*p < 0.05, **p < 0.01 ***p < 0.001. Abbreviations: HPTLC, high-performance thin-layer chromatography.

Table 3 Ponatinib increases markers of inflammation

Treatment	Dose	BAL fluid		Urinary ureum/ creatinine ratio	MCP-1	SAA	E-selectin
	mg/kg	*Protein (µg/mL)*	*Albumin (µg/mL)*		*pg/mL*	*µg/mL*	*ng/mL*
Baseline	-	-	-	-	45 ± 23	6.8 ± 4.4	87 ± 9
Control	-	405 ± 291	243 ± 168	12.4 ± 4.6	102 ± 44†	10.1 ± 1.2	96 ± 18
Imatinib	150	330 ± 176	192 ± 94	20.5 ± 9.6	54 ± 44	9.6 ± 0.5	71 ± 18
Nilotinib	10	400 ± 207	235 ± 126	10.5 ± 8.8	144 ± 82‡	10.6 ± 1.0	79 ± 23
	30	265 ± 103	168 ± 66	10.1 ± 2.6	117 ± 60‡	10.6 ± 1.1	99 ± 17
Ponatinib	3	198 ±75*	129 ± 54	12.3 ± 6.0	78 ± 29	10.4 ± 1.9	77 ± 22
	10	215 ± 61*	144 ± 38	158.2 ± 371.9	92 ± 68	15.2 ± 21.1†	250 ± 307**/‡

Effect of imatinib, nilotinib and ponatinib on BAL fluid, urinary ureum/creatinine ratio and inflammatory markers as measured at baseline (t=0 weeks) and after 16 weeks of treatment. Data are presented as means ± SD (n = 8–15 per group).*p<0.05, **p<0.001 as compared to control, †p<0.05, ‡p<0.001 as compared to baseline. Abbreviations: BAL, broncho-alveolar lavage; MCP-1, monocyte chemoattractant protein-1; SAA, serum amyloid A.

Ponatinib increases plasma E-selectin

Inflammation is widely considered as an important contributing factor to cardiovascular events (41). Therefore, we measured plasma levels of macrophage-derived chemokine MCP-1, the adhesion molecule E-selectin as marker of endothelial activation, and SAA, an acute phase protein mainly produced by the liver (**Table 3**). None of the inflammatory markers were significantly altered by imatinib. The WTD increased MCP-1 relative to baseline (t=0 weeks) (+126%, p=0.015), as did nilotinib (10 mg/kg, +220%, p<0.001; 30 mg/kg, +160%, p<0.001). Ponatinib increased SAA relative to baseline (+123%, p=0.013), but not relative to control. In four of the fifteen ponatinib-treated mice, E-selectin levels were 3 to 10 times increased, leading to an overall increase of 161% (p<0.001) when compared to control, which may point to endothelial activation by ponatinib. Collectively, these data confirm the safety profile of imatinib and suggest endothelial activation and potential endothelial dysfunction in some animals by ponatinib.

Atherosclerosis

Imatinib and ponatinib reduce lesion size and severity

Next we analyzed the effects of long-term exposure of the anti-CML TKIs on the progression of atherosclerosis as a cardiovascular endpoint, as shown by representative images (**Figure 3**). Sixteen weeks of WTD resulted in the development of 4.0 ± 0.8 atherosclerotic lesions and 156 ± 61*1 000 µm^2 lesion area per cross-section in the control group (**Figure 4A**). Approximately 55% of these lesions were severe (type IV–V) lesions and only 10% of the segments were unaffected (**Figure 4B**). The total number of lesions was not

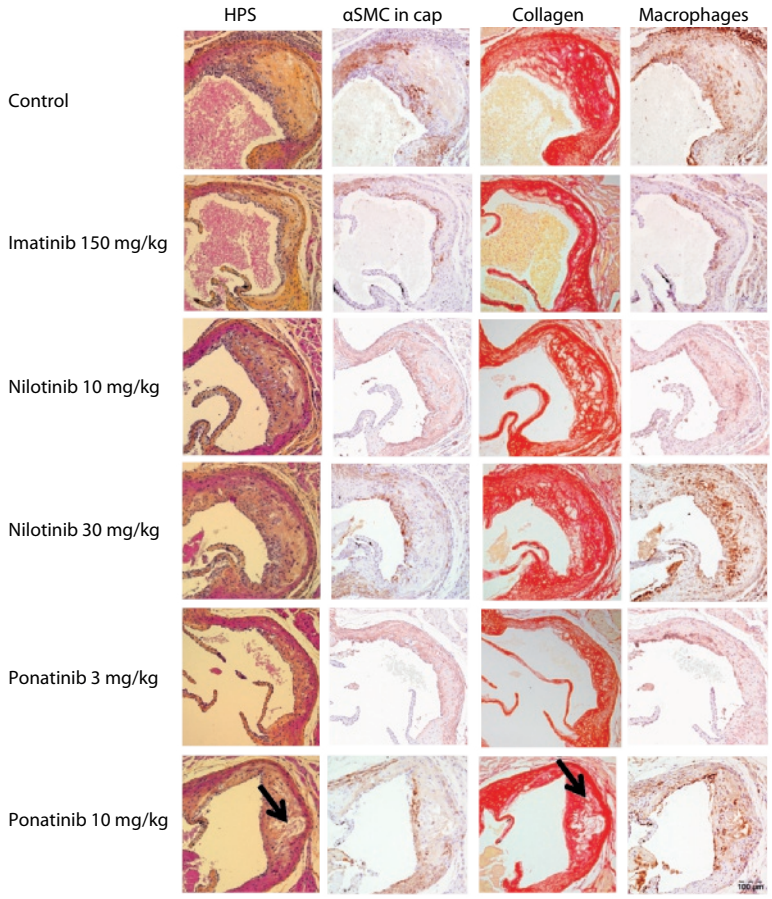

Figure 3 Effect of imatinib, nilotinib and ponatinib on plaque composition. Representative images of HPS staining, immunostaining with α-actin for SMCs, Sirius red staining for collagen and immunostaining with Mac-3 for macrophages. The arrows depict necrotic areas, including cholesterol clefts. Abbreviations: HPS, hematoxylin-phloxine-saffron; SMCs, smooth muscle cells; MAC-3, Purified anti-mouse CD107b Mac-3 Antibody.

affected by any treatment (data not shown), but imatinib and ponatinib diminished the lesion area by 78% ($p<0.001$), 52% (3 mg/kg, $p=0.002$), and 48% (10 mg/kg, $p=0.006$), respectively (**Figure 4A**). In addition, the total lesion area that consisted of severe lesions was reduced by imatinib (–56%, $p<0.001$) (**Figure 4B**). Next, we evaluated whether this anti-atherogenic effect of imatinib and ponatinib could be explained by the reduction in plasma cholesterol levels. The square root of the lesion size was positively correlated with

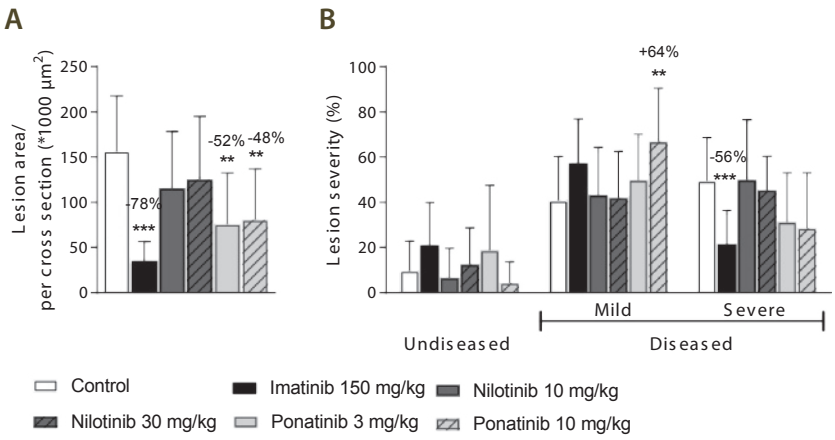

Figure 4 Imatinib and ponatinib reduce atherosclerotic progression. After 16 weeks of treatment, the total lesion area per cross-section was assessed (A). Lesion severity was assessed, categorized as no lesions/undiseased, mild lesions (type I-III) and severe lesions (type IV-V) and expressed as percentage of total lesion area. (B). Data are presented as means ± SD (n=13–15 per group).**p<0.01 ***p<0.001.

plasma cholesterol exposure (mmol/L*weeks) in control, imatinib and high dose nilotinib and ponatinib treated mice (control R^2=0.79, p=0.001; imatinib R^2=0.71, p=0.003; ponatinib 10 mg/kg R^2=0.79, p<0.001; nilotinib 30 mg/kg R^2=0.63, p=0.016) (**Figure 5**). Lesion size per cross-section was not correlated with inflammation markers or blood pressure, indicating a dominant role of plasma cholesterol and cholesterol-lowering by the drugs in the development of atherosclerosis.

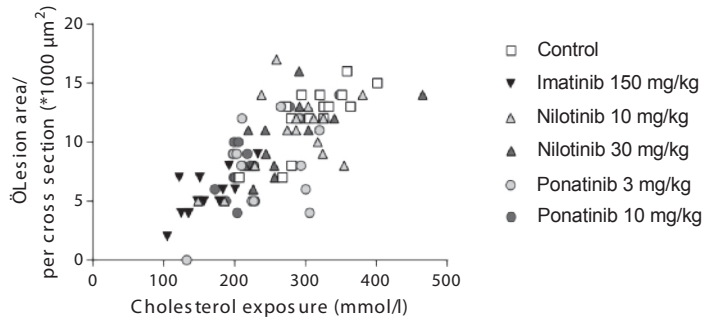

Figure 5 Atherosclerotic lesion area is correlated with cholesterol exposure. Correlation between cholesterol exposure (mmol/L*weeks) and the square root of the lesion area was calculated with a Pearsons's correlation test (n=13–15 per group).

Imatinib improves plaque morphology

To assess the plaque phenotype as a marker for vulnerability to rupture, lesion morphology was analyzed in the type IV and V lesions from mice treated with imatinib and the high dosages of nilotinib and ponatinib, as shown by representative images (**Figure 3**). The macrophage and necrosis content were quantified as factors that decrease plaque stability, and smooth muscle cell area in the cap of the lesions and collagen as factors that improve plaque stability (17,26,31) (**Figure 6A**). Average macrophage, necrotic core, collagen and αSMC content in the control group were 24 ± 8%, 4 ± 2%, 42 ± 10% and 4 ± 3%, respectively (**Figure 6A**). Imatinib increased the collagen content by 47% (62 ± 17%, p=0.004) and tended to increase αSMC content (+38%, p=0.050), resulting in an enhanced lesion stability index (+216%, p=0.004) (**Figure 6B**). Nilotinib (10 mg/kg) decreased collagen content (–32%, p=0.003), resulting in a decreased lesion stability index (–43%, p=0.003). Ponatinib (3 mg/kg) decreased necrotic core content (–58%, p=0.001) without affecting plaque stability. Collectively, these data indicate that imatinib induces a more stable plaque phenotype with collagen-rich lesions.

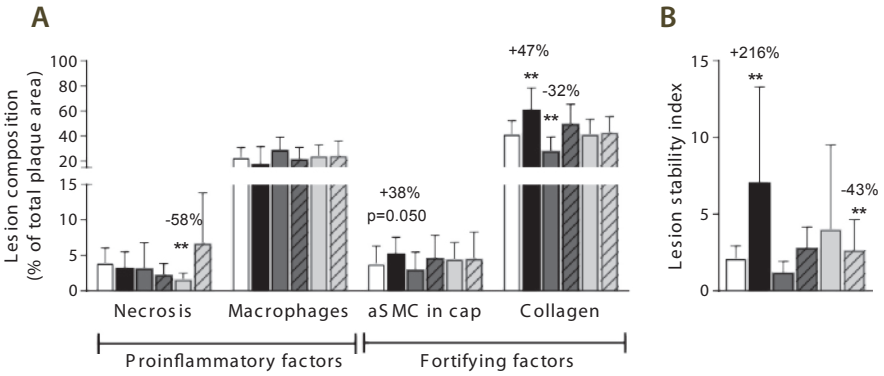

Figure 6 Imatinib increases plaque stability. Necrotic and macrophage content as pro-inflammatory factors, and αSMCs and collagen as fortifying factors, were determined in the severe (type IV-V) lesions and expressed as percentage of total plaque area (A). Plaque stability index was calculated (B). Data are presented as means ± SD (n=13–15 per group). **p<0.01. Abbreviations: aSMC; α smooth muscle cells.

Transcriptome analysis

Ponatinib adversely alters gene expression of coagulation factors

To find early molecular signatures of other clinically relevant processes induced by the anti-CML drugs, gene expression and pathway analysis was performed in the liver as the central organ in lipid metabolism and synthesis of coagulation factors. To identify drug-specific molecular responses and overlap between the various treatments, the total

number of differentially expressed genes (DEGs) was assessed and a Venn-diagram was constructed comprising all DEGs compared to control group. Both ponatinib and nilotinib displayed a dose-dependent increase in the total number of DEGs as compared to control and the molecular response of the high-dose ponatinib had more overlapping genes with imatinib than nilotinib (**Figure 7**).

General categorization of biological functions showed that all anti-CML drugs affect canonical pathways associated with mitochondrial dysfunction and oxidative phosphorylation, most likely induced by oxidative stress and leading to reduced energy production, and processes involved in protein synthesis and cell growth (EIF2 signaling), confirming the target-related molecular responses of anti-CML drugs. (**Figure 8**).

The processes relevant to (cardio)vascular (side) effects of the anti-CML drugs are highlighted in **Figure 9** and **Figure 10**. Although gene expression data from the liver cannot be directly extrapolated to atherosclerosis signaling in the vascular wall, gene expression profiles of different organs have affiliation with each other and may be predictive for these biological processes. Therefore, the transcriptome data of the liver as predicting organ are given. As compared to the other TKI's, imatinib showed the most pronounced effects on atherosclerosis signaling, with favorable regulation of genes involved in cell adhesion (*Integrin β2* and *α4, Icam1, Vcam1, Psgl-1*), macrophage activation (*Cd40, Tnfrsf14, Scara1, Nfκb*), lipid regulation (*Lpl, Apoa1, Apoa2, Apoc2, Apoc4, Pla2g7*), inflammatory processes (*Cd40, Nfκb, Il1a, Tnfrsf14, Icam1, Vcam1*) and genes related to extracellular matrix modulation (*Col1a2, Col3a1, Col1a1, Mmp13, Tgf-β*) (**Figure 9**). Ponatinib showed similar effects, but to a lesser extent, whereas these effects were not observed after nilotinib treatment (**Figure 9**).

As the site of synthesis of a large number of coagulation factors, the liver plays an important role in the regulation of hemostatic and thrombotic processes. Although all three TKIs to some extent affected the coagulation pathways, ponatinib had the most adverse profile (**Figure 10**). Ponatinib increased the gene expression of members of the intrinsic or contact activation pathway, *Kng1a* and *Klkb1*, mainly involved in growth of a thrombus, and of the extrinsic or tissue factor pathway *F7*, involved in initiation of thrombus formation, and decreased gene expression of *Upa* and *Tpa*, both involved in fibrinolysis. Nilotinib showed down-regulation of the expression of *F5*, *F9*, and *Protein S*, while *Serpina1* (PAI-1) was up-regulated. Imatinib down-regulated the expression of *Upa*, *Tpa* and *Protein S* and up-regulated *Serpina1* and *Protein C*. This analysis demonstrates that among the three anti-CML drugs investigated ponatinib most prominently induces adverse alterations in the gene expression of coagulation factors in both the intrinsic and extrinsic pathway, which may lead to a state of hypercoagulability.

A

	Number of differentially expressed genes versus control group				
	Imatinib 150 mg/kg BID	Nilotinib 10 mg/kg QD	Nilotinib 30 mg/kg QD	Ponatinib 3 mg/kg QD	Ponatinib 10 mg/kg QD
Imatinib 150 mg/kg BID	1575	224	417	213	670
Nilotinib 10 mg/kg QD		474	313	41	248
Nilotinib 30 mg/kg QD			1066	78	484
Ponatinib 3 mg/kg QD				504	235
Ponatinib 10 mg/kg QD					1344

B

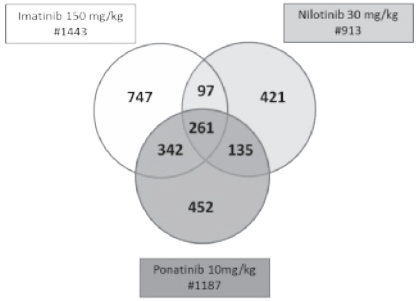

C

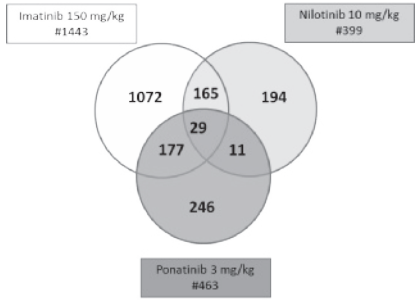

Figure 7 Overview of differentially expressed genes (DEGs). The numbers in the diagonal display DEG compared to control. The numbers above the diagonal indicate the number of DEGs shared between the treatment groups. Bayes pvalues of <0.01 were used as cut-off (A). To evaluate which biological processes are affected with the various treatments, all genes (p<0.01) were uploaded in the Ingenuity Pathway Analysis (IPA) tool to perform gene set enrichments. The number of differentially expressed genes that are annotated in IPA are indicated in Venn-diagrams (B-C). This number is slightly different between A and B-C since the RNA-seq method also detects genes that are not yet annotated in the IPA database (n=8 per group).

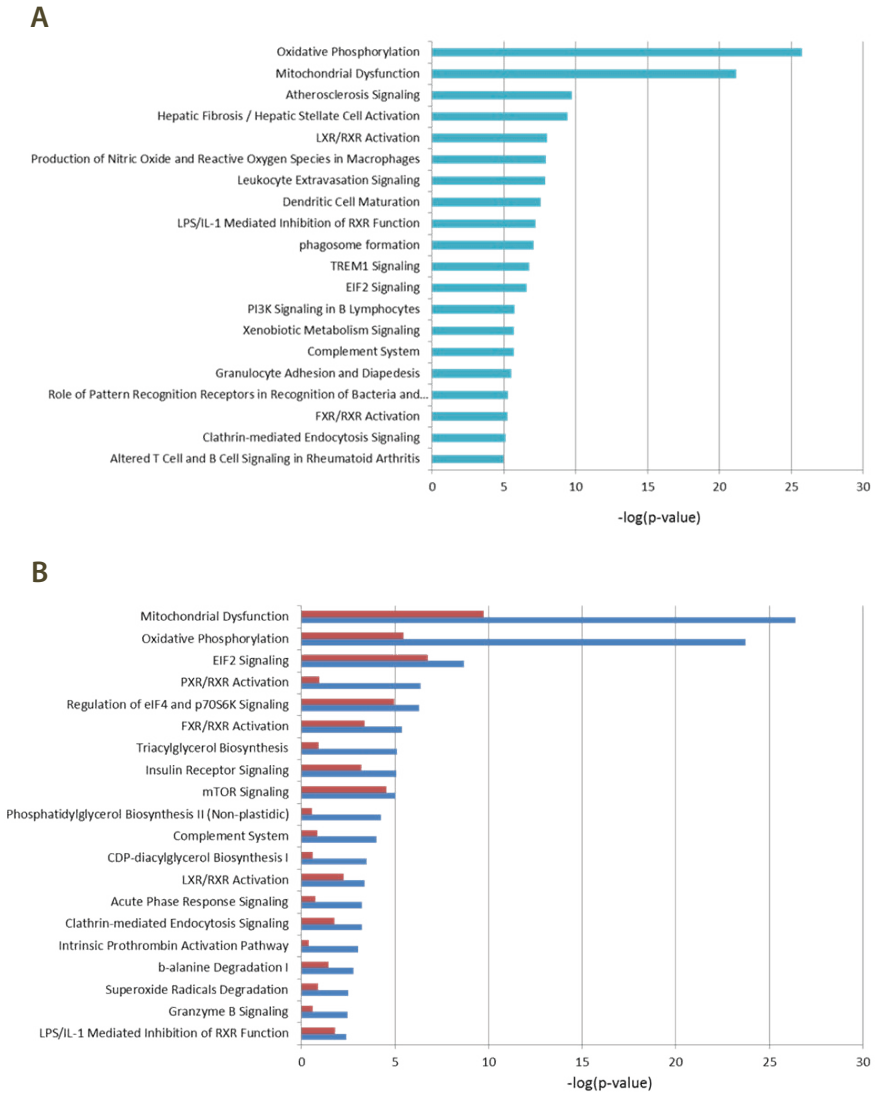

Figure 8 To identify the most relevant processes affected by TKI treatment, we calculated the canonical biological processes/ pathways affected by imatinib 150 mg/kg (A), nilotinib 10 mg/kg (red bars) and 30 mg/kg (blue bars) (B) and by ponatinib 3 mg/kg (red bars) and 10 mg/kg (blue bars) (C). The relevance of each process is indicated by a pvalue of overlap. The p-value of overlap is calculated based on Fisher's exact test which is set standard for overlap analysis in IPA-software. For visualization purposes the –log of the p-value of the top 20 processes are plotted on the x-axes (n=8 per group).

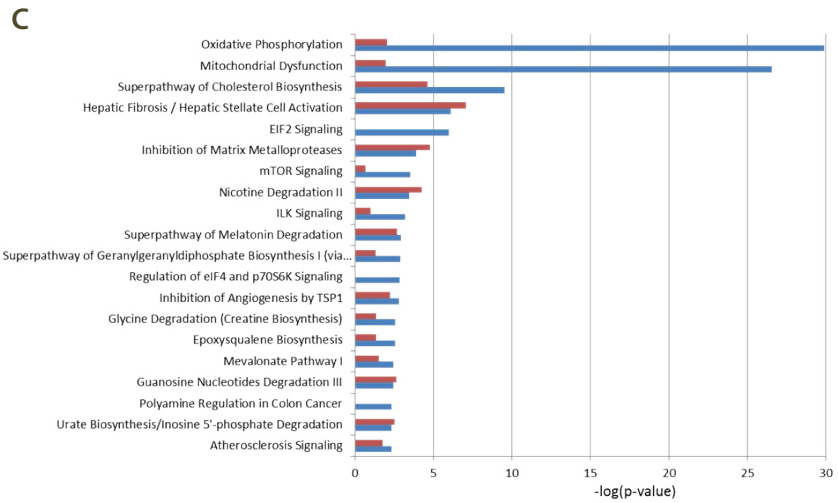

Figure 8 Continued.

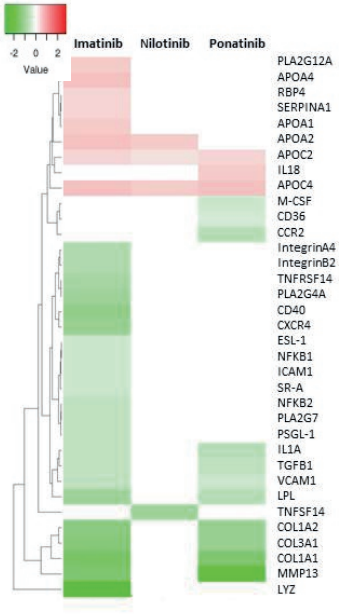

Figure 9 TKI treatment regulates many genes related to atherosclerosis signaling, with the most pronounced effect by imatinib. The heat map shows all significantly upregulated (red) and down-regulated (green) genes involved in atherosclerosis signaling of mice treated with imatinib (150 mg/kg), nilotinib (30 mg/kg) or ponatinib (10 mg/kg) as compared to control mice. P-values of <0.01 were used as cut-off (n=8 per group).

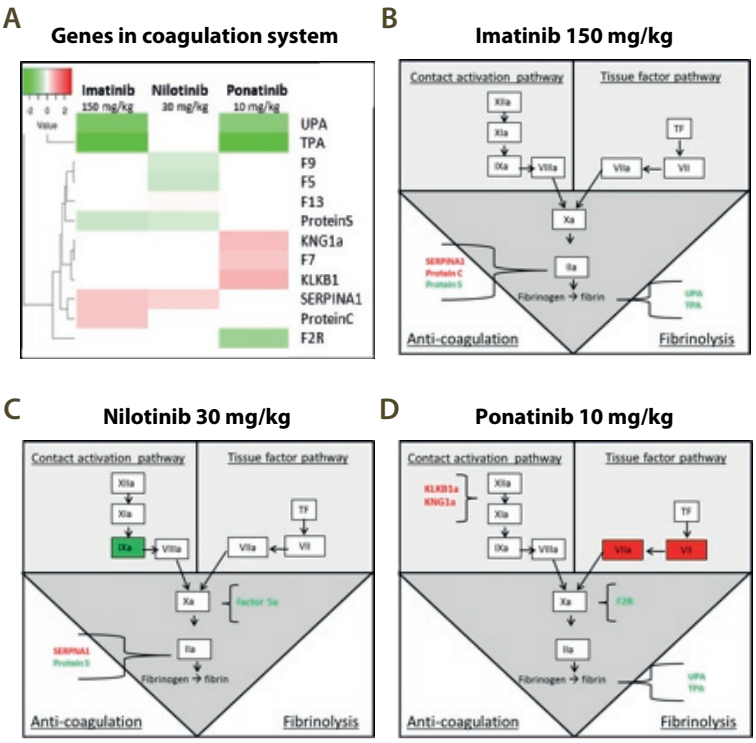

Figure 10 Genes in the coagulation system regulated by imatinib, nilotinib and ponatinib. The heat map shows all significantly ($p<0.01$) upregulated (red) and downregulated (green) genes involved in coagulation of mice treated with imatinib (150 mg/kg), nilotinib (30 mg/kg) or ponatinib (10 mg/kg) as compared to control mice (A). Imatinib regulates genes involved in anti-coagulation and fibrinolysis (B). Factor 9a and 5a were down-regulated and SERPINA1 up-regulated by nilotinib (C). Ponatinib showed the most adverse profile with upregulation of genes in both the contact activation and tissue factor pathway, together with downregulation of genes involved in fibrinolysis (D). pvalues of <0.01 were used as cut-off (n=8 per group).

Coagulation

Ponatinib increases plasma factor VII and nilotinib increases factor VIIa activity

Next, we measured total factor VII coagulant activity (FVII) and VIIa activity (FVIIa) in plasma. Ponatinib increased FVII after 4 weeks (10 mg/kg, +265%, $p<0.001$) and 12 weeks of treatment (3 mg/kg, +28%, $p=0.07$; 10 mg/kg + 82%, $p<0.001$) (**Figure 11A**). In addition, nilotinib increased the activity of FVIIa at 4 weeks by 82% (30 mg/kg, $p<0.001$) (**Figure 11B**). Together, these data confirm our findings on gene expression analysis and reveal the pro-thrombotic characteristics of nilotinib and ponatinib.

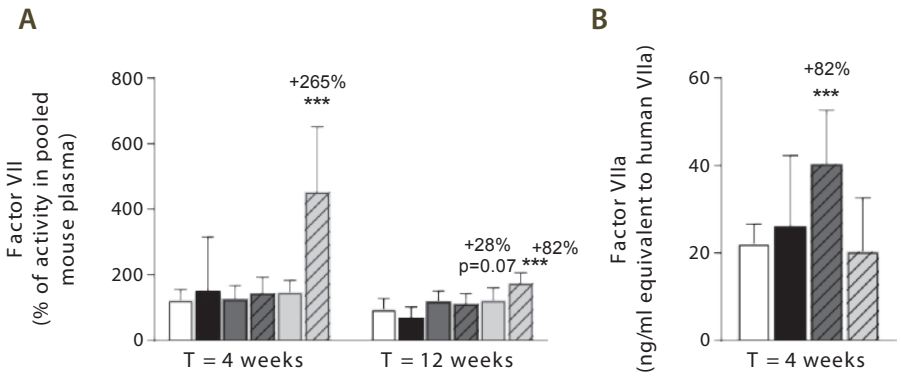

Figure 11 Ponatinib increases factor VII and nilotinib increases factor VIIa activity. Factor VII was measured after 4 and 12 weeks of treatment as the percentage of activity in reference pooled mouse plasma (A). Factor VIIa activity was measured after 4 weeks of treatment (B). Data are presented as means ± SD (n=6–20 per group).***p<0.001.

Discussion

This is the first study that compared the effect of a first, second and third generation BCR-ABL1 tyrosine kinase inhibitor on (cardio)vascular risk factors and atherosclerosis. Imatinib and ponatinib decreased plasma cholesterol and atherosclerosis, while nilotinib and ponatinib activated coagulation. The pharmacokinetic data we provide enabled us to use drug exposures translatable to CML-patients and can be used to optimize future TKI research. In addition, we provide a robust data set obtained by gene expression and pathway analysis of the liver, which predicted that ponatinib may lead to a pro-coagulant state by adversely affecting coagulation factors of both the contact activation (intrinsic) and tissue factor (extrinsic) pathways, which was confirmed by increased levels of the coagulation factor VII. In addition, nilotinib increased activity of FVIIa. These findings can be used by clinicians to carefully monitor coagulation parameters in CML-patients to predict risk of cardiovascular events.

The choice to perform this study in a non-leukemic mouse model has several reasons. First, there is, inherent to the diagnosis and progression of the disease, a shortage of suitable high quality plasma samples of CML patients collected at both baseline and follow-up under similar conditions. Second, CML affects both metabolic (10) and coagulation (11) parameters which makes it difficult to elucidate the role of TKI treatment on the reported VAEs independently of the underlying disease. Last, we were able to investigate a broad range of parameters, including atherosclerosis and gene expression and pathway analysis of the liver, which is not possible in CML-patients.

Imatinib and ponatinib, but not nilotinib, decreased plasma cholesterol contained in the pro-atherogenic apoB-containing lipoproteins. Cholesterol reduction and even normalization in hypercholesterolemic CML-patients is repeatedly described in retrospective studies with CML-patients for imatinib (37–39,42) and is consistent with our findings. Data on ponatinib are scarce (42) and it is unclear whether nilotinib affects plasma cholesterol in CML-patients. Some studies reported increased plasma cholesterol (5,8,40,42), whereas others question this (43). These opposing findings may be explained by the response to the underlying disease. It should be noted that nilotinib is often prescribed as a second-line treatment after resistance to imatinib. Reduced caloric intake induced by the leukemia and increased energy requirements imposed by tumor growth may result in lower cholesterol levels at baseline, while a positive response to treatment is often accompanied by increased cholesterol levels in oncologic patients (44). This response-related cholesterol elevation may be abolished by the cholesterol-lowering effects of imatinib and ponatinib per se as found in our study, resulting in decreased (imatinib) or normalized (ponatinib) plasma cholesterol levels in CML patients.

Several mechanisms are involved in cholesterol homeostasis, including intestinal uptake, hepatic uptake and secretion as lipoproteins, synthesis and storage, and fecal excretion. The decreased hepatic lipid content in imatinib and ponatinib treated mice (**Figure 2**) points to a shortage of cholesterol in the liver and suggests that not lipoprotein clearance, but VLDL production and/or intestinal absorption of cholesterol are affected by imatinib and ponatinib. Indeed, when myeloid tumor cells are treated with imatinib, de novo fatty acid synthesis is reduced, pointing towards decreased VLDL particle production (45). However, besides the shared activity of TKIs used for CML-treatment against the BCR-ABL1 tyrosine kinase, the potency and activity to affect off-target kinases differs markedly, and thus different processes may be involved. To our knowledge, no *in vivo* studies are available that investigated the effects of TKI treatment on cholesterol and lipoprotein metabolism, and functional studies are required.

Important observations from our study are the reduced development of atherosclerosis by imatinib and ponatinib which was correlated to decreased plasma cholesterol levels, and the increased plaque stability induced by imatinib, which has not been reported previously by others. There are no reports that describe the effect of ponatinib on atherosclerosis development in an animal model, and there are inconsistent reports on imatinib and nilotinib. In line with our findings, imatinib reduced atherosclerosis in STZ-induced diabetic ApoE$^{-/-}$ mice (46) and high fat fed ApoE$^{-/-}$ mice (47), though lesion reduction was independent of plasma cholesterol lowering and attributed to vascular wall remodeling and reduced inflammation. Interestingly, and in contrast with previous (46–48) and the present findings, Hadzijusufovic et al (49). did not find an effect of imatinib on atherosclerosis in ApoE$^{-/-}$ mice, but reported increased atherosclerosis by nilotinib. In addition, a direct pro-atherogenic effect on human endothelial cells was found, as shown by upregulation of adhesion factors ICAM-1, E-selectin and VCAM-1 (49), which is in line with the increase of

markers of endothelial activation found in CML patients treated with nilotinib (50). Unfortunately, no data on plasma cholesterol and markers of endothelial activation in the mice were provided. We do not have a clear explanation for the discrepancy with our findings, but the use of different animal models and dosages, as well as the underlying disease may play a role.

Ponatinib increased plasma E-selectin and urinary albumin/creatinine in some animals, suggesting endothelial activation and potential endothelial dysfunction, wherein aberrant angiogenesis might be involved. Indeed, an *in vitro* study using human umbilical vein endothelial cells (HUVECs) demonstrated the potential of ponatinib to reduce endothelium viability, and to induce apoptosis, reduce migration, inhibit tube formation, and to negatively affect endothelial progenitor cell function, all important for angiogenesis (51). In addition, ponatinib reduced von Willebrand factor (vWF) expression on lung endothelial cells in rats (52), which is an interesting finding, because vWF is not only a specific marker for endothelial cells, but also functions in coagulation.

Although there were no clinical signs of thrombosis or bleeding in our long-term study, an unbiased and exploratory transcriptome analysis revealed that ponatinib treatment lead to a pro-thrombotic state by affecting important players in the activation of the coagulation pathway. Ponatinib increased gene expression of *Klkb1*, *Kng1a* (part of the intrinsic or contact activation pathway) and *F7* (part of the extrinsic or tissue factor pathway) and decreased expression of *Upa* and *Tpa*, which function in resolution of thrombi by fibrinolysis. Consistent with the increased gene expression, plasma levels of factor VII were increased by 265%. Nilotinib had less pronounced effects on gene expression of coagulation factors but increased activity of FVIIa by 82%. Using a different experimental design, Alhawiti et al. (50) recently reported that a single dose of nilotinib but not imatinib increased platelet aggregation and thrombus growth *ex vivo* and *in vivo* in mice, and increased *ex vivo* platelet adhesion and thrombin generation in CML-patients receiving nilotinib (50). On the other hand, Loren et al. (53) demonstrated that ponatinib, but not imatinib and nilotinib, inhibited *ex vivo* human platelet activation, spreading and aggregation, and hypothesized that the cardiovascular events observed in patients treated with ponatinib may be the result of effects on other organs and cell types. Indeed, we show that FVII is involved, which is produced by the liver, and is an important factor in the coagulation pathway. Mice lacking FVII have delayed thrombus formation (54) and pharmacological doses of rFVIIa induce hemostasis in severe hemophilia and in non-hemophilia patients with profuse, heavy bleeding (55). Collectively, these data indicate that nilotinib and ponatinib can both potentiate a pro-thrombotic state via different mechanisms of action.

The presence of one or more risk factors for (cardio)-metabolic disease together with the increased platelet aggregation and increased plasma activity of factor VII/VIIa may contribute to the onset of thrombosis, especially when combined with increased levels of tissue factor (TF), which activates the TF pathway (**Figure 10**). Hypercoagulability has been described in a variety of malignancies, including hematological malignancies (55,56), and many tumor cells express high levels of TF, the primary initiator of the extrinsic

coagulation pathway (57). Therefore, we propose that nilotinib and ponatinib induce (athero) thrombosis in a subgroup of CML-patients through a combination of (cardio)-metabolic risk factors, enhanced levels of TF and increased plasma levels of coagulation factors. Our findings can be used to develop a multivariate risk model for CVD in CML patients, which include (cardio) vascular risk factors and coagulation parameters at baseline and during treatment, facilitating an early detection strategy for patients prone to cardiovascular events, which will improve therapy decision and patient care.

In conclusion, using a comprehensive approach to measure the cardiovascular effects of various BCR-ABL1 inhibitors, we demonstrate that first, second and third generation BCR-ABL1 inhibitors have very distinct effects on lipid metabolism, blood coagulability and atherosclerosis. The first-generation inhibitor imatinib was proven safe, with evident benefit for plasma lipid concentrations, atherosclerotic plaque size and stability. The third-generation inhibitor ponatinib showed similar, albeit less pronounced effects on lipid concentrations and atherosclerosis, but also showed a hypercoagulable phenotype. These data perfectly match retrospective clinical observations on cardiovascular effects of BCR-ABL1 inhibitors, and besides providing a biological basis for these observations, may well contribute to safer application of these drugs in the future.

Acknowledgments

The authors thank Anne Kozijn (TNO) for her help with the FACS analysis, Joost Westerhout (TNO) for the analysis of the pharmacokinetics and Kees van Leuven (GBS) for performing the measurements of coagulation factors.

Disclosures

C.K. has ownership interests in 'Good Biomarker Sciences'. R.G. is an employee at Bristol-Meyers Squibb, New York, USA. J.W.J. received research grants from and has spoken at (CME-accredited) meetings sponsored by Amgen, Astellas, Astra-Zeneca, Daiichi Sankyo, Lilly, Merck-Schering-Plough, Pfizer, Roche, Sanofi-Aventis, the Netherlands Heart Foundation, the Interuniversity Cardiology Institute of the Netherlands, and the European Community Framework KP7 Program.

The remaining authors declare that the research was conducted in the absence of any commercial or financial relationships that could be constructed as a potential conflict of interest.

Funding

This work was supported in part by Bristol-Meyers Squibb, New York, USA, by an allowance for TKI-LSH from the Ministry of Economic Affairs in the Netherlands (TKI1413P01), the TNO research program "Preventive Health Technologies" and the European Union Seventh Framework Programme (FP7/2007-2013) grant nr. 602936 (CarTarDis project). JA is funded by the Dutch Heart Foundation (Grant number 2014T064).

References

1. de Klein A, van Kessel AG, Grosveld G, et al. A cellular oncogene is translocated to the Philadelphia chromosome in chronic myelocytic leukaemia. Nature. 1982 Dec;300(5894):765–7.
2. Druker BJ, Guilhot F, O'Brien SG, et al. Five-year follow-up of patients receiving imatinib for chronic myeloid leukemia. N Engl J Med. 2006 Dec;355(23):2408–17.
3. O'Hare T, Walters DK, Stoffregen EP, et al. In vitro activity of Bcr-Abl inhibitors AMN107 and BMS-354825 against clinically relevant imatinib-resistant Abl kinase domain mutants. Cancer Res. 2005 Jun;65(11):4500–5.
4. Cortes JE, Kim D-W, Pinilla-Ibarz J, et al. A phase 2 trial of ponatinib in Philadelphia chromosome-positive leukemias. N Engl J Med. 2013 Nov;369(19):1783–96.
5. Castagnetti F, Breccia M, Gugliotta G, et al. Nilotinib 300 mg twice daily: an academic single-arm study of newly diagnosed chronic phase chronic myeloid leukemia patients. Haematologica. 2016 Oct;101(10):1200–7.
6. Moslehi JJ, Deininger M. Tyrosine Kinase Inhibitor-Associated Cardiovascular Toxicity in Chronic Myeloid Leukemia. J Clin Oncol. 2015 Dec;33(35):4210–8.
7. Valent P, Hadzijusufovic E, Schernthaner G-H, et al. Vascular safety issues in CML patients treated with BCR/ABL1 kinase inhibitors. Blood. 2015 Feb;125(6):901–6.
8. Kim TD, Rea D, Schwarz M, et al. Peripheral artery occlusive disease in chronic phase chronic myeloid leukemia patients treated with nilotinib or imatinib. Leukemia. 2013 Jun;27(6):1316–21.
9. Tefferi A. Nilotinib treatment-associated accelerated atherosclerosis: when is the risk justified? Vol. 27, Leukemia. England; 2013. p. 1939–40.
10. Muller CP, Wagner AU, Maucher C, et al. Hypocholesterolemia, an unfavorable feature of prognostic value in chronic myeloid leukemia. Eur J Haematol. 1989 Sep;43(3):235–9.
11. Wehmeier A, Daum I, Jamin H, et al. Incidence and clinical risk factors for bleeding and thrombotic complications in myeloproliferative disorders. A retrospective analysis of 260 patients. Ann Hematol. 1991 Aug;63(2):101–6.
12. van der Hoogt CC, de Haan W, Westerterp M, et al. Fenofibrate increases HDL-cholesterol by reducing cholesteryl ester transfer protein expression. J Lipid Res. 2007 Aug;48(8):1763–71.
13. de Haan W, van der Hoogt CC, Westerterp M, et al. Atorvastatin increases HDL cholesterol by reducing CETP expression in cholesterol-fed APOE*3-Leiden.CETP mice. Atherosclerosis. 2008 Mar;197(1):57–63.
14. van der Hoorn JWA, de Haan W, Berbee JFP, et al. Niacin increases HDL by reducing hepatic expression and plasma levels of cholesteryl ester transfer protein in APOE*3Leiden.CETP mice. Arterioscler Thromb Vasc Biol. 2008 Nov;28(11):2016–22.
15. Ason B, van der Hoorn JWA, Chan J, et al. PCSK9 inhibition fails to alter hepatic LDLR, circulating cholesterol, and atherosclerosis in the absence of ApoE. J Lipid Res. 2014 Nov;55(11):2370–9.
16. Kuhnast S, van der Hoorn JWA, Pieterman EJ, et al. Alirocumab inhibits atherosclerosis, improves the plaque morphology, and enhances the effects of a statin. J Lipid Res. 2014 Oct;55(10):2103–12.
17. Kuhnast S, van der Tuin SJL, van der Hoorn JWA, et al. Anacetrapib reduces progression of atherosclerosis, mainly by reducing non-HDL-cholesterol, improves lesion stability and adds to the beneficial effects of atorvastatin. Eur Heart J. 2015 Jan;36(1):39–48.
18. Dewey FE, Gusarova V, Dunbar RL, et al. Genetic and Pharmacologic Inactivation of ANGPTL3 and Cardiovascular Disease. N Engl J Med. 2017 Jul;377(3):211–21.
19. de Vries-van der Weij J, de Haan W, Hu L, et al. Bexarotene induces dyslipidemia by increased very low-density lipoprotein production and cholesteryl ester transfer protein-mediated reduction of high-density lipoprotein. Endocrinology. 2009 May;150(5):2368–75.
20. van Vlijmen BJ, van 't Hof HB, Mol MJ, et al. Modulation of very low density lipoprotein production and clearance contributes to age- and gender- dependent hyperlipoproteinemia in apolipoprotein E3-Leiden transgenic mice. J Clin Invest. 1996 Mar;97(5):1184–92.
21. Groot PH, van Vlijmen BJ, Benson GM, et al. Quantitative assessment of aortic atherosclerosis in APOE*3 Leiden transgenic mice and its relationship to serum cholesterol exposure. Arterioscler Thromb Vasc Biol. 1996 Aug;16(8):926–33.

22. Trion A, de Maat MPM, Jukema JW, et al. No effect of C-reactive protein on early atherosclerosis development in apolipoprotein E*3-leiden/human C-reactive protein transgenic mice. Arterioscler Thromb Vasc Biol. 2005 Aug;25(8):1635–40.
23. Kleemann R, Verschuren L, van Erk MJ, et al. Atherosclerosis and liver inflammation induced by increased dietary cholesterol intake: a combined transcriptomics and metabolomics analysis. Genome Biol. 2007; 8(9):R200.
24. Verschuren L, Radonjic M, Wielinga PY, et al. Systems biology analysis unravels the complementary action of combined rosuvastatin and ezetimibe therapy. Pharmacogenet Genomics. 2012 Dec;22(12):837–45.
25. Kooistra T, Verschuren L, de Vries-van der Weij J, et al. Fenofibrate reduces atherogenesis in ApoE*3Leiden mice: evidence for multiple antiatherogenic effects besides lowering plasma cholesterol. Arterioscler Thromb Vasc Biol. 2006 Oct;26(10):2322–30.
26. Kuhnast S, van der Hoorn JWA, van den Hoek AM, et al. Aliskiren inhibits atherosclerosis development and improves plaque stability in APOE*3Leiden.CETP transgenic mice with or without treatment with atorvastatin. J Hypertens. 2012 Jan;30(1):107–16.
27. Post SM, Zoeteweij JP, Bos MH, et al. Acyl-coenzyme A:cholesterol acyltransferase inhibitor, avasimibe, stimulates bile acid synthesis and cholesterol 7alpha-hydroxylase in cultured rat hepatocytes and in vivo in the rat. Hepatology. 1999 Aug;30(2):491–500.
28. Delsing DJ, Offerman EH, van Duyvenvoorde W, et al. Acyl-CoA:cholesterol acyltransferase inhibitor avasimibe reduces atherosclerosis in addition to its cholesterol-lowering effect in ApoE*3-Leiden mice. Circulation. 2001 Apr;103(13):1778–86.
29. Stary HC, Chandler AB, Dinsmore RE, et al. A definition of advanced types of atherosclerotic lesions and a histological classification of atherosclerosis. A report from the Committee on Vascular Lesions of the Council on Arteriosclerosis, American Heart Association. Circulation. 1995 Sep;92(5):1355–74.
30. Landlinger C, Pouwer MG, Juno C, et al. The AT04A vaccine against proprotein convertase subtilisin/kexin type 9 reduces total cholesterol, vascular inflammation, and atherosclerosis in APOE*3Leiden.CETP mice. Eur Heart J. 2017 Aug;38(32):2499–507.
31. Kuhnast S, Louwe MC, Heemskerk MM, et al. Niacin Reduces Atherosclerosis Development in APOE*3Leiden. CETP Mice Mainly by Reducing NonHDL-Cholesterol. PLoS One. 2013;8(6):e66467.
32. Tan SY, Kan E, Lim WY, et al. Metronidazole leads to enhanced uptake of imatinib in brain, liver and kidney without affecting its plasma pharmacokinetics in mice. J Pharm Pharmacol. 2011 Jul;63(7):918–25.
33. Peng B, Hayes M, Resta D, et al. Pharmacokinetics and pharmacodynamics of imatinib in a phase I trial with chronic myeloid leukemia patients. J Clin Oncol. 2004 Mar;22(5):935–42.
34. European Medicines Agency. Scientific Discussion on Tasigna I-N. No Title [Internet]. 2007. Available from: http://www.ema.europa.eu/docs/en_GB/document_library/EPAR_-_Scientific_Discussion/human/000798/WC500034398.pdf
35. European Medicines Agency. ANNEX I. Summary of product characteristics Iclusig INN-ponatinib. No Title [Internet]. Available from: http://www.ema.europa.eu/docs/en_GB/document_library/EPAR_-_Product_Information/human/002695/WC500145646.pdf
36. FDA. Clinical pharmacology and biopharmaceutics; Inclusig. [Internet]. 2012. Available from: https://www.accessdata.fda.gov/drugsatfda_docs/nda/2012/203469Orig1s000ClinPharmR.pdf
37. Gottardi M, Manzato E, Gherlinzoni F. Imatinib and hyperlipidemia. Vol. 353, The New England journal of medicine. United States; 2005. p. 2722–3.
38. Franceschino A, Tornaghi L, Benemacher V, et al. Alterations in creatine kinase, phosphate and lipid values in patients with chronic myeloid leukemia during treatment with imatinib. Vol. 93, Haematologica. Italy; 2008. p. 317–8.
39. Gologan R, Constantinescu G, Georgescu D, et al. Hypolipemiant besides antileukemic effect of imatinib mesylate. Leuk Res. 2009 Sep;33(9):1285–7.
40. Hochhaus A, Saglio G, Hughes TP, et al. Long-term benefits and risks of frontline nilotinib vs imatinib for chronic myeloid leukemia in chronic phase: 5-year update of the randomized ENESTnd trial. Leukemia. 2016 May;30(5):1044–54.
41. Libby P. Inflammation in atherosclerosis. Arterioscler Thromb Vasc Biol. 2012 Sep;32(9):2045–51.

42. Rea D, Mirault T, Cluzeau T, et al. Early onset hypercholesterolemia induced by the 2nd-generation tyrosine kinase inhibitor nilotinib in patients with chronic phase-chronic myeloid leukemia. Haematologica. 2014 Jul;99(7):1197–203.
43. Breccia M, Loglisci G, Cannella L, et al. Nilotinib therapy does not induce consistent modifications of cholesterol metabolism resulting in clinical consequences. Vol. 35, Leukemia research. England; 2011. p. e215-6.
44. Baroni S, Scribano D, Zuppi C, et al. Prognostic relevance of lipoprotein cholesterol levels in acute lymphocytic and nonlymphocytic leukemia. Acta Haematol. 1996;96(1):24–8.
45. Boren J, Cascante M, Marin S, et al. Gleevec (STI571) influences metabolic enzyme activities and glucose carbon flow toward nucleic acid and fatty acid synthesis in myeloid tumor cells. J Biol Chem. 2001 Oct;276(41):37747–53.
46. Lassila M, Allen TJ, Cao Z, et al. Imatinib attenuates diabetes-associated atherosclerosis. Arterioscler Thromb Vasc Biol. 2004 May;24(5):935–42.
47. Ballinger ML, Osman N, Hashimura K, et al. Imatinib inhibits vascular smooth muscle proteoglycan synthesis and reduces LDL binding in vitro and aortic lipid deposition in vivo. J Cell Mol Med. 2010 Jun;14(6B):1408–18.
48. El-Agamy DS. Nilotinib attenuates endothelial dysfunction and liver damage in high-cholesterol-fed rabbits. Hum Exp Toxicol. 2017 Nov;36(11):1131–45.
49. Hadzijusufovic E, Albrecht-Schgoer K, Huber K, et al. Nilotinib-induced vasculopathy: identification of vascular endothelial cells as a primary target site. Leukemia. 2017 Nov;31(11):2388–97.
50. Alhawiti N, Burbury KL, Kwa FA, et al. The tyrosine kinase inhibitor, nilotinib potentiates a prothrombotic state. Thromb Res. 2016 Sep;145:54–64.
51. Gover-Proaktor A, Granot G, Shapira S, et al. Ponatinib reduces viability, migration, and functionality of human endothelial cells. Leuk Lymphoma. 2017 Jun;58(6):1455–67.
52. Kang Z, Ji Y, Zhang G, et al. Ponatinib attenuates experimental pulmonary arterial hypertension by modulating Wnt signaling and vasohibin-2/vasohibin-1. Life Sci. 2016 Mar;148:1–8.
53. Loren CP, Aslan JE, Rigg RA, et al. The BCR-ABL inhibitor ponatinib inhibits platelet immunoreceptor tyrosine-based activation motif (ITAM) signaling, platelet activation and aggregate formation under shear. Thromb Res. 2015 Jan;135(1):155–60.
54. Xu Z, Lioi J, Mu J, et al. A multiscale model of venous thrombus formation with surface-mediated control of blood coagulation cascade. Biophys J. 2010 May;98(9):1723–32.
55. Elice F, Rodeghiero F. Hematologic malignancies and thrombosis. Thromb Res. 2012 Mar;129(3):360–6.
56. Simkovic M, Vodarek P, Motyckova M, et al. Venous thromboembolism in patients with chronic lymphocytic leukemia. Thromb Res. 2015 Dec;136(6):1082–6.
57. Falanga A. Thrombophilia in cancer. Semin Thromb Hemost. 2005 Feb;31(1):104–10.